Eur Respir J 2008; 32: 854–861
DOI: 10.1183/09031936.00141007

Frequency and peak stretch magnitude affect alveolar epithelial permeability

T.S. Cohen, K.J. Cavanaugh and S.S. Margulies

ABSTRACT: The present study measured stretch-induced changes in transepithelial permeability to uncharged tracers (1.5–5.5 Å) using cultured monolayers of alveolar epithelial type-I like cells. Cultured alveolar epithelial cells were subjected to uniform cyclic (0, 0.25 and 1.0 Hz) biaxial stretch from 0% to 12, 25 or 37% change in surface area (ΔSA) for 1 h.

Significant changes in permeability of cell monolayers were observed when stretched from 0% to 37% ΔSA at all frequencies, and from 0% to 25% ΔSA only at high frequency (1 Hz), but not at all when stretched from 0% to 12% ΔSA compared with unstretched controls. At stretch oscillation amplitudes of 25 and 37% ΔSA, imposed at 1 Hz, tracer permeability increased compared with that at 0.25 Hz. Cells subjected to a single stretch cycle at 37% ΔSA (0.25 Hz), to simulate a deep sigh, were not distinguishable from unstretched controls.

Reducing stretch oscillation amplitude while maintaining a peak stretch of 37% ΔSA (0.25 Hz) *via* the application of a simulated post-end-expiratory pressure did not protect barrier properties.

In conclusion, peak stretch magnitude and stretch frequency were the primary determining factors for epithelial barrier dysfunction, as opposed to oscillation amplitude.

KEYWORDS: Barrier properties, tight junction, ventilator-induced lung injury

Ventilator-induced lung injury (VILI), produced by cyclic overinflation and collapse of airways and alveoli, is characterised by markers of reduced alveolar epithelial and/or endothelial barrier function, such as air leaks, pulmonary oedema and alveolar flooding [1].

A recent clinical study on ventilation strategies was carried out by the ARDSnet and showed mortality rates of patients with acute respiratory distress syndrome decreased significantly (22%) when a low (6 mL·kg^{-1}) tidal volume (V_T) was used compared with standard V_T (12 mL·kg^{-1}) [2]. Often, increased ventilation frequency is used to preserve minute ventilation at low V_T and positive end-expiratory pressure (PEEP) is used to prevent alveolar collapse during mechanical ventilation. In the ARDSnet study ventilation frequency was controlled to maintain blood pH (7.3–7.4), and was ~0.5 and 0.25 Hz for the low and high V_T groups, respectively [2]. In addition, PEEP was maintained at ~8.5 and ~9.4 cmH_2O (0.83 and 0.92 kPa) for the low and high V_T groups, respectively [2]. It is possible that the higher PEEP used in the high V_T group may have contributed to the poor outcome.

A second ARDSnet clinical trial compared two PEEP levels (~8 and ~13 cmH_2O; 0.8 and 1.3 kPa) at the same V_T (6.0 mL·kg^{-1}), and revealed no protective or deleterious effects of increased PEEP for low stretch oscillation amplitude (SOA) ventilation [3]. Rate was controlled to maintain a pH of >7.30 and averaged ~0.5 Hz for both groups. There are, however, questions about this second study, specifically concerning how study parameters were changed mid-trial, yet all data were combined and used [4]. In summary, the use of PEEP is still a widely discussed issue, with >280 studies on this topic being published in the last 2 yrs alone.

While both the epithelium and endothelium serve as barriers to particulate and fluid motion into the alveolus, the epithelium provides much more resistance to alveolar flooding [5]. A relationship between epithelial stretch and inspired lung volume in intact lungs has been previously identified [6]. Herein, the present authors propose that both large stretch magnitudes and frequencies adversely affect epithelial barrier properties, including permeability.

An *in vitro* primary cell monolayer model of the alveolar epithelium that mimics lung inflation has been developed [6, 7]. Briefly, equibiaxial stretch is applied to change the surface area of the monolayer at controlled frequencies and magnitudes. In a previous study, cultured monolayers were cyclically stretched at one stretch rate

For editorial comments see page 826.

AFFILIATIONS
Dept of Bioengineering, University of Pennsylvania, Philadelphia, PA, USA.

CORRESPONDENCE
S.S. Margulies
Dept of Bioengineering
210 South 33rd St
University of Pennsylvania
Philadelphia
PA 19104-6321
USA
Fax: 1 2155732071
E-mail: margulie@seas.upenn.edu

Received:
October 25 2007
Accepted after revision:
June 24 2008

SUPPORT STATEMENT
This study was supported by a National Heart, Lung, and Blood Institute grant (no. NIH R01 HL-57204).

STATEMENT OF INTEREST
None declared.

European Respiratory Journal
Print ISSN 0903-1936
Online ISSN 1399-3003

(0.25 Hz) to magnitudes of 25 or 37% change in surface area (ΔSA). It was concluded that only epithelial deformation to magnitudes of 37% ΔSA, corresponding to 100% total lung capacity (TLC), created a disruption of barrier properties to uncharged molecular tracers (radii 1.5–5.5 Å) [6, 8]. These data concurred with findings by EGAN [9, 10] who showed that static inflation of whole sheep and rabbit lungs to 100% TLC produced permeability increases to tracers (radii 14–34 Å), while smaller inflations did not.

In the current study, an *in vitro* model is used to study the effects of mechanical stretch frequency, stretch oscillation amplitude and peak stretch magnitude on barrier properties. To better understand the affect of PEEP on VILI, a combination of tonic stretch (PEEP component) and cyclic stretch (ventilation component) was applied to other isolated epithelial monolayers. The present study complements a previous cell viability study [11] and expands on a previous functional study [8] that investigated epithelial permeability under stretch conditions, which was designed to mimic ventilation of the intact rodent respiratory system with moderate and high PEEP (at ~13 and ~35 cmH_2O; 1.3 and 3.4 kPa) and higher frequencies of ventilation [12]. The current study demonstrates that large peak stretch magnitude and high frequencies increase the flux of uncharged tracers into the alveolus, and that caution should be applied when combining the two in a clinical setting.

MATERIALS AND METHODS

Cell isolation

Primary rat alveolar epithelial type-II cells were isolated from pathogen-free male Sprague-Dawley rats (250–350 g) *via* an elastase digestion technique adopted from DOBBS *et al.* [13]. After isolation, cells were resuspended in a solution of minimum essential minerals, 10% foetal bovine serum (FBS), 0.4 $\mu L \cdot mL^{-1}$ gentamicin and 1 $\mu L \cdot mL^{-1}$ amphotericin B (Life Technologies, Rockville, MD, USA) and seeded (1×10^6 $cells \cdot cm^{-2}$) on permeable co-polyester membranes (Mylan Technologies, Burlington, VT, USA) mounted in custom-built polysulphone wells. Prior to the experiment, the membrane was corona discharge-treated and coated with poly-L-lysine (0.5 $\mu g \cdot cm^{-2}$; Sigma, St. Louis, MO, USA) and fibronectin (10 $\mu g \cdot cm^{-2}$; Boehringer Mannheim Biochemicals, Indianapolis, IN, USA) to improve cell adhesion. Wells were incubated for a period of 5 days, during which the media was changed daily. Other studies have previously shown that following 5–6 days in culture, type-II alveolar epithelial cells seeded on fibronectin and maintained with 10% FBS adopt type-I features [7, 14–16]. Another study noted that permeable supports encourage emergence of type-I features and non-permeable supports inhibit transformation [17]. To confirm this phenotypic transformation, even on this elastic impermeable construct, cells were embedded in Epon A12 (Electron Microscopy Supply, Port Washington, NY, USA) and sectioned (60–85 nm). The cells were examined using electron microscopy after 2 and 5 days in culture (fig. 1). Although cells at day 2 (fig. 1a) contained numerous lamellar bodies, by day 5 cells seeded on the fibronectin-coated elastic substrate had formed monolayers and phenotypic characteristics of type-I cells, including tight junctions (fig. 1b) and loss of lamellar bodies (fig. 1c). Furthermore, cells seeded on fibronectin-coated permeable constructs developed transepithelial resistances averaging 800–1,000 $\Omega \cdot cm^2$, values representative of properly formed confluent alveolar monolayers [18, 19].

Cell monolayer stretching protocol

Wells were washed with Ringer's solution (NaCl 126.4 mM, $NaHCO_3$ 25 mM, HEPES 15 mM, glucose 5.55 mM, KCl 5.4 mM, $CaCl_2$ 1.8 mM, $MgSO_4$ 0.81 mM, NaH_2PO_4 0.78 mM; pH 7.4) and mounted in a custom-made stretch device capable of applying a uniform and equibiaxial stretch to the cells at a user-defined magnitude and frequency [7]. In a 3×3 design, wells were stretched at one of three frequencies (1, 0.25 or 0 Hz) and at one of three magnitudes (12, 25 or 37% ΔSA) for 1 h. In the present study, 0 Hz was defined as a prolonged constant stretch held for 1 h. The three stretch magnitudes correspond to the strains experienced by the alveolar epithelium *in vivo* at inflations from functional residual capacity to 70, 90 and 100% TLC, or V_T of 15, 25 and 30 $mL \cdot kg^{-1}$, respectively, in a rat with no PEEP [6]. Additional wells were stretched cyclically (0.25 Hz) from 12 to 25% or 25 to 37% ΔSA for 1 h, corresponding to lung stretch *in vivo* from 70–90% and 90–100% TLC, respectively. In rats with an intact chest wall, these two stretch paradigms would be associated with PEEP-SOA combinations of ~13 cmH_2O PEEP, 10 mL per kg body weight SOA and 35 cmH_2O PEEP, 5 mL per kg body weight SOA, respectively [20]. The final experimental group was subjected to a single stretch of 37% ΔSA at a frequency of 0.25 Hz to elicit the effect of a large ''sigh'' to TLC (with 2 s inspiration, 2 s expiration). The remainder of the wells were left unstretched in the device to serve as unstretched, time-matched controls. A total of 24 wells were used at each stretch condition for each tracer. The temperature of the stretch device was maintained at 37°C.

Cell monolayer tracer transport measurements

After the 1-h experimental period, wells were removed from the stretch device and mounted into Ussing chambers within ~2 min. The apical-to-basal paracellular permeability of the monolayers was assessed using a previously described tracer transport method [8]. Briefly, five dextrorotary oligopeptide tracers were used to measure permeability: alanine (molecular radius 2.2 Å), valine (2.8 Å), alanine-alanine (3.6 Å), alanine-alanine-alanine (4.4 Å), and leucine-leucine (5.5 Å). Tracer radius was estimated from molecular models obtained from the Protein Data Bank [21]. Tracer transport in the apical-to-basal direction was measured over a 2-h period using a separate tracer for each well. Tracer samples (100 μL) were removed from the basal chamber every 30 min and replaced with fresh Ringer's solution. Tracer concentrations were assessed by mixing a basal fluid sample with fluorescamine and quantifying the fluorescence using a microplate fluorimeter (Thermo Labsystems, Vantaa, Finland) with an excitation filter of 405 nm and an emission filter of 485 nm.

Diffusive paracellular transport of tracers was assumed, with no sources or sinks and using well-established equations governing conservation of mass [22, 23]. Transport for each tracer followed first-order Fickian diffusion described by equation 1:

$$\ln\left(\frac{C_{ap0} - \left(1 + \frac{V_B}{V_{ap}}\right)C_B(t)}{C_{ap0} - \left(1 + \frac{V_B}{V_{ap}}\right)C_{B0}}\right) = -\frac{\left(1 + \frac{V_B}{V_{ap}}\right)PS}{V_B}(t - t_0) \quad (1)$$

where C_{ap0} is the initial apical tracer concentration, C_{B0} the

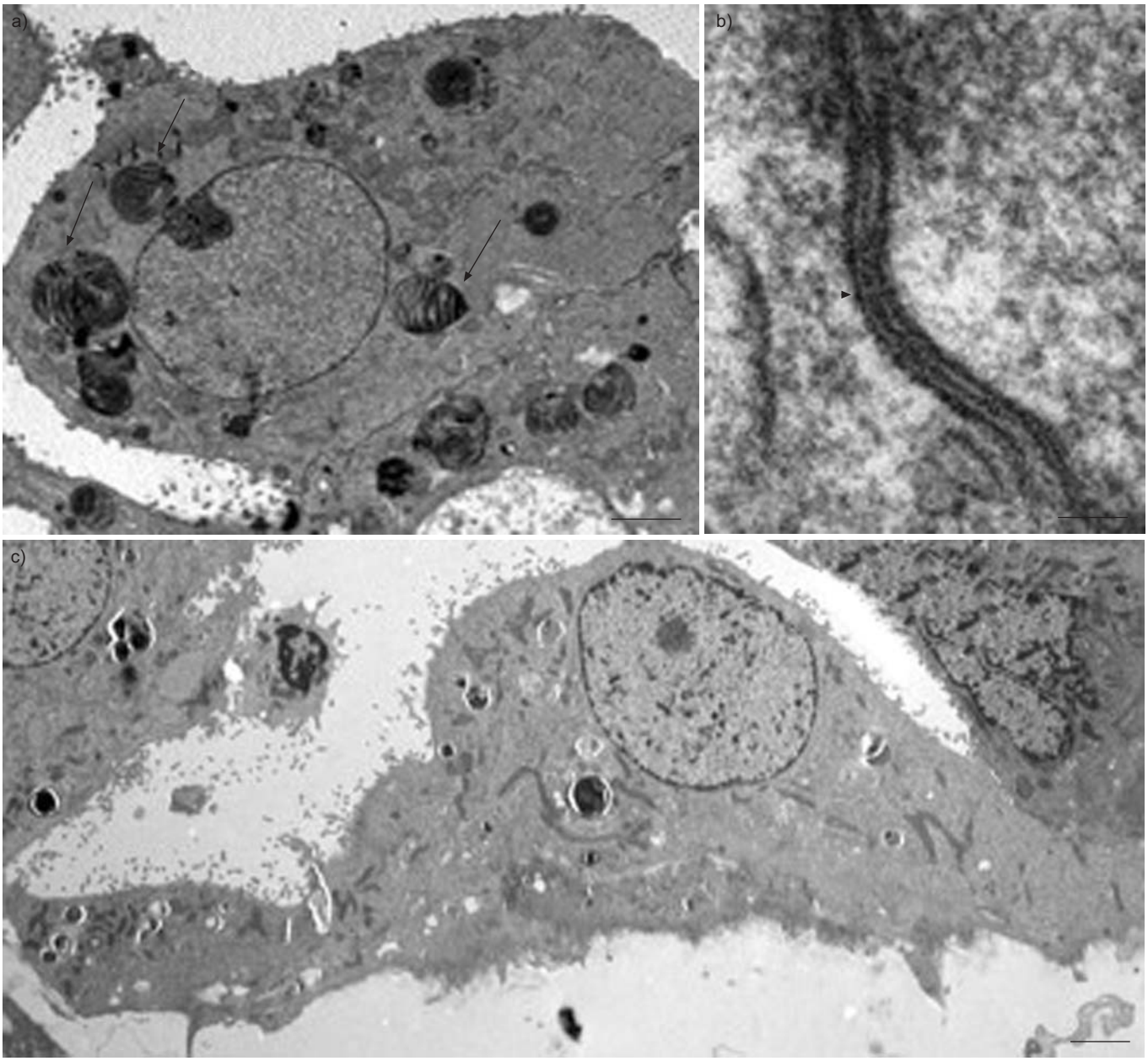

FIGURE 1. Electronmicrographs of rat alveolar type-II cells seeded on fibronectin-coated elastic substrate and maintained for a) 2 days in culture showing numerous lamellar bodies (arrows). b and c) After 5 days in culture, cells take on an alveolar type-I ''like'' phenotype (c) with no lamellar bodies but the formation of tight junctions (b; arrowhead). a and c) Scale bars=2 μm. b) Scale bar=5 nm.

initial basal tracer concentration and $C_B(t)$ the basal concentration at time t. The paracelullar permeability of the monolayer to a specific tracer (units=length/time) is represented by P, S is the surface area over which transport occurs, t_0 the initial time, V_{ap} is the apical volume and V_B is basal volume. P was calculated over each of the four post-stretch or post-control periods (t=30, 60, 90 and 120 min), and modelled as a piecewise continuous function. The Tukey's test for significance determined that tracer permeability was not a function of the time at which the sample was drawn [24], and p-values determined from samples across time were averaged to yield p-values for each tracer (for each well) as a result of the applied stretch regimen.

Calculation of equivalent pore radius

The calculated permeability values for all the tracers were used to develop a model of the equivalent pore radii of the epithelium as a function of applied stretch, as previously described [8]. Based on the two-pore model by KIM and CRANDALL and co-workers [25, 26], paracellular tracer flux can be represented by equation 2:

$$PS = D((A_{PS}/dx)f(a/r_S) + (A_{PL}/dx)f(a/r_L)) \quad (2)$$

where D is the diffusion coefficient of the tracer in water, A_{PS} and A_{PL} are the total pore area of the membrane for small and

large pores, respectively, dx is the length of the cylindrical pores, a is the tracer radius, r_S and r_L are the pore radii for small and large pores, respectively, and *P* and *S* are defined as in equation 1. The polynomial function f(a/r) is defined by equation 3, and represents the steric hindrance to molecular diffusion:

$$f(a/r) = (1 - a/r^2)(1 - 2.10a/r + 2.09a/r^3 - 0.95a/r^5) \quad (3)$$

To compute the pore radii, the authors first defined alanine-alanine (3.6 Å) as the reference tracer, based on observations from previous calculations using a single pore model, and used permeability data for tracers greater than or equal to the reference to solve for larger pore radii, and permeability data for tracers smaller than the reference to solve for small pore radii. Furthermore, it was assumed that the large tracers were unable to pass through small pores and, therefore, could neglect large tracer transport through the small pores when solving for large pore radii. In addition, A_{PL} and A_{PS} were calculated from these equations using the calculated pore radii and the reference permeability value. The number of pores was calculated using equations 4 and 5 for large and small pores, respectively:

$$n = A_{PL}/\pi r_L^2 \quad (4)$$

$$n = A_{PS}/\pi r_S^2 \quad (5)$$

Statistical analysis

To determine the effect of stretch frequency on paracellular permeability in cultured monolayers, separate permeability analyses for each tracer were performed, comparing across frequencies at a particular stretch magnitude using ANOVA. Subsequently, *post hoc* Tukey's tests were used for multiple comparisons [24]. Statistical significance was defined as $p \leqslant 0.05$.

Specifically, *in vitro* monolayer tracer permeabilities measured in the 12–25% ΔSA and 25–37% ΔSA stretch groups (0.25 Hz), were compared with each other and previously obtained tracer data from a 0.25 Hz 0–12% ΔSA stretch group (0.25 Hz; Tukey's test) to evaluate differences between these three stretch strategies that employed 12–13% ΔSA cyclic SOAs [8].

The final analysis of the *in vitro* monolayer data was used to determine whether the peak deformation magnitude or the SOA of stretch is the main determinant of barrier disruption in these cells. The 12–25% ΔSA (0.25 Hz) group was compared with the previously obtained 0–25% ΔSA (0.25 Hz) group using an unpaired t-test [24]. Similarly, data from the 25–37% ΔSA (0.25 Hz) stretch group were compared with those of the previously examined 0–37% ΔSA (0.25 Hz) group to examine the same phenomena at higher stretch magnitudes.

RESULTS

In a previous study it has been shown that paracellular permeability of cultured alveolar epithelial cells stretched cyclically at 0.25 Hz significantly increased compared with that of unstretched cells, but only with a stretch from 0% to 37% ΔSA not with 0% to 25% ΔSA [8]. It was, therefore, concluded that at stretch magnitudes $\geqslant$37% ΔSA (100% TLC), sustained low-frequency cycling can damage barrier properties.

In the current study, the same tracers were used to evaluate the effect of mechanical conditions analogous to clinical ventilation paradigms on epithelial permeability. It was found that increasing stretch cycling frequency to 1 Hz increased the permeability of cultured monolayers stretched from 0% to 37% ΔSA (fig. 2). Specifically, passive transport of all tracers through monolayers stretched from 0% to 37% ΔSA at 1 and 0.25 Hz was significantly greater than that through unstretched monolayers, and transport at 1 Hz was also significantly greater than passive transport of most tracers under 0 Hz stretch to 37% ΔSA (fig. 2). Moreover, for cyclic stretch from 0% to 37% ΔSA, permeability at 1 Hz was even significantly greater than for stretch at 0.25 Hz for two tracers (fig. 2). Even a 0 Hz stretch held at 37% ΔSA for 1 h significantly increased the permeability for valine (2.8 Å) and alanine-alanine (3.6 Å) compared with unstretched monolayers (fig. 2). However, sustained 0 Hz and cyclic stretch to 37% ΔSA can damage barrier properties. The present authors found that a single sigh, a brief stretch at a rate of 0.25 Hz to 37% ΔSA (100% TLC or 30 mL·kg^{-1} in the rat), did not significantly increase the permeability of cell monolayers to any of the tracers compared with unstretched controls (fig. 2).

Similar to stretch at 37% ΔSA, permeability of monolayers stretched to 25% ΔSA at a frequency of 1 Hz was also significantly greater than unstretched cells for all tracers (fig. 3), and even greater than the permeability of monolayers stretched at 0 Hz or 0.25 Hz at 25% ΔSA for all but the smallest tracer (fig. 3). From the current data at both 25% and 37% ΔSA, it can be concluded that stretch frequency is an important determinant of barrier dysfunction at $\geqslant$25% ΔSA (90% TLC or 25 mL·kg^{-1} in the *in vivo* rat).

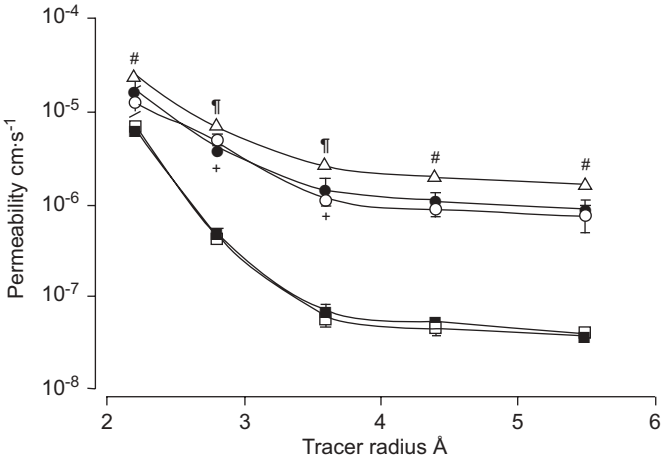

FIGURE 2. Permeability of monolayers stretched to 37% change in surface area at frequencies ranging 0–1 Hz. The tracers used were: alanine (2.2 Å), valine (2.8 Å), alanine-alanine (3.6 Å), alanine-alanine-alanine (4.4 Å) and leucine-leucine (5.5 Å). Unstretched and 0.25 Hz data have been presented previously [8]. □: unstretched; ■: single stretch 0.25 Hz; ○: 0 Hz; ●: 0.25 Hz; △: 1 Hz. #: $p<0.05$ for cells stretched at 1 Hz, tracer permeabilities were significantly different from those of the unstretched group and the 0 Hz group; ¶: $p<0.05$ for cells from the unstretched group and the 0 Hz and 0.25 Hz groups; +: $p<0.05$ for the 0 Hz group, tracer permeabilities were different from those of unstretched cells.

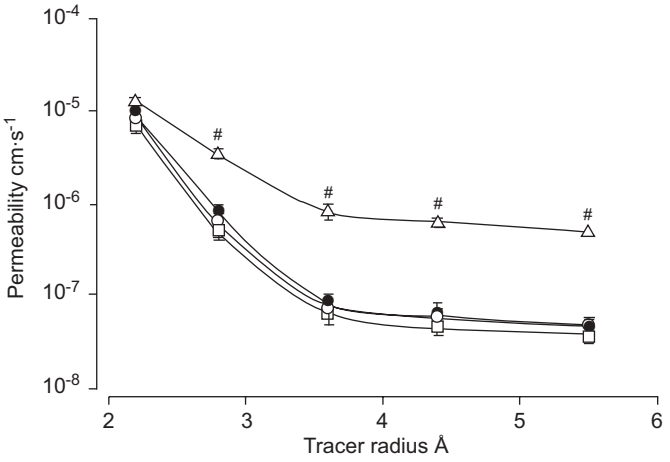

FIGURE 3. Permeability of monolayers stretched to 25% change in surface area at frequencies ranging 0–1 Hz. The tracers used were: alanine (2.2 Å), valine (2.8 Å), alanine-alanine (3.6 Å), alanine-alanine-alanine (4.4 Å) and leucine-leucine (5.5 Å). Unstretched and 0.25 Hz data have been presented previously [8]. □: unstreched; ○: 0 Hz; ●: 0.25 Hz; ■: 1 Hz. #: $p<0.0001$, tracer permeabilities were different from those of unstretched cells and the cells stretched at 0 and 0.25 Hz.

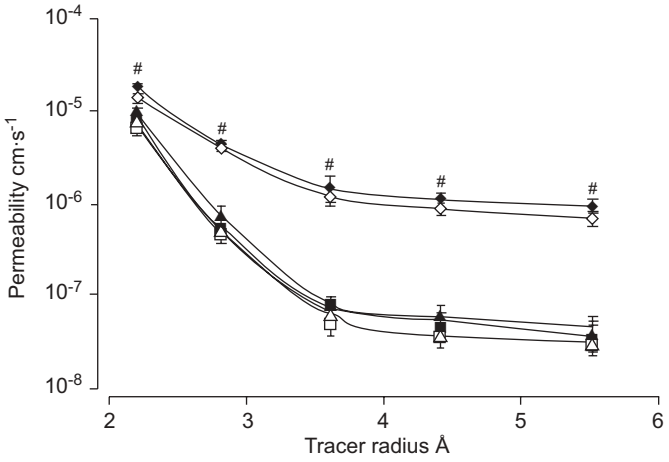

FIGURE 4. Influence of simulated positive end-expiratory pressure on permeability of monolayers stretched cyclically. The tracers used were: alanine (2.2 Å), valine (2.8 Å), alanine-alanine (3.6 Å), alanine-alanine-alanine (4.4 Å) and leucine-leucine (5.5 Å). □: unstretched; ■: 0–12% change in surface area (ΔSA); △: 12–25% ΔSA; ▲: 0–25% ΔSA; ◇: 25–37% ΔSA; ◆: 0–37% ΔSA. #: $p<0.005$ for cells stretched between 25–37% ΔSA, tracer permeabilities were significantly different from the 0–12% and the 12–25% ΔSA group.

To determine if sustained cycling from a minimum, nonzero, stretch magnitude compromised barrier properties of monolayers exposed to small (12 or 13% ΔSA) SOAs, permeability of monolayers cycled at either 12–25% ΔSA or 25–37% ΔSA (0.25 Hz) were examined and the values compared to those of monolayers cycled at the same SOA (0–12% ΔSA), but with no pre-stretch or PEEP (fig. 4). Assuming this minimum stretch magnitude of 12% ΔSA is similar to an end-expiratory stretch, this magnitude corresponds to an end-expiratory pressure equivalent to ~13 cmH_2O (1.3 kPa) in the intact respiratory system [6]. The combination of this moderate, nonzero minimum stretch (PEEP) with an SOA from 70–90% TLC (10 $mL \cdot kg^{-1}$ in the rat) did not alter monolayer permeability to any tracer (fig. 4; 12–25% ΔSA). However, in the 25–37% ΔSA group, the combination of a minimum stretch of 25% ΔSA (or PEEP of 35 cmH_2O (3.4 kPa) in the intact respiratory system) with an SOA from 90–100% TLC (5 $mL \cdot kg^{-1}$ in the rat), which is independently a noninjurious SOA, significantly increased permeability to all tracers (fig. 4; 25–37% ΔSA). However, when SOA was reduced to zero and the same large PEEP equivalent stretch (25% ΔSA) was applied and held at constant (0 Hz) stretch for 1 h (fig. 4), permeability did not increase relative to unstretched controls. Thus, it can be concluded that PEEP alone was not the cause of the increased permeability of monolayers stretched from 25–37% ΔSA, but rather peak stretch magnitude was primarily responsible. Permeability increased significantly only when maximum stretch reached 37% ΔSA (or 100% TLC) either tonically or dynamically.

To determine if SOA affected the influence of peak stretch magnitude on permeability, two sets of data were examined comparing conditions with matched maximum stretch at a frequency of 0.25 Hz: 12–25% ΔSA with 0–25% ΔSA, and 25–37% ΔSA with 0–37% ΔSA. No significant differences were found between groups stretched to the same peak magnitude.

As a theoretical basis for interpreting the changes in monolayer permeability following stretch, the monolayers were modelled as an impermeable sheet with two populations of pores, a large radius and small radius population, available for tracer transport. The model was fit to permeability data obtained from each of the five tracers following each stretch regimen, and pore radii, total pore area and pore number were calculated (table 1). In a previous study, this model was used to show that following a cycling rate of 0.25 Hz, only stretch to 37% ΔSA produced increases in small (two-fold) and large (nine-fold) pore radius compared with unstretched values [8]. Furthermore, at this stretch magnitude and rate a decrease in total area occupied by small pores was reported (to 32% of unstretched) and an increase in the total area of large pores was reported (to 1,976% of unstretched). In the present study, the total area occupied by both small and large pores at the same rates and magnitudes was demonstrated; however, the large pore area increased most, with dramatic increases at 37% ΔSA.

The present study also examined high rates of cyclic stretch (1.0 Hz) to 25% and 37% ΔSA, as well as the effect of cyclic stretch with PEEP (12–25% and 25–37% ΔSA at 0.25 Hz). Comparing stretch at 37% ΔSA at 1.0 Hz to 0.25 Hz, both small and large pore size increased, but increases in total small pore area were smaller (two- and four-fold, respectively) than large pore area (39- and 22-fold, respectively, compared with unstretched monolayers). The further increase in permeability for small tracers, seen by increasing the rate to 1.0 Hz (fig. 2), seems to be related to increases in total area of the large pores. This relationship also holds at 25% ΔSA, where the large and small pore area increases are less than at 37% ΔSA at the same frequencies, but again the significant increase in large and small tracer permeability at 1.0 Hz (fig. 3) seems to correlate with the 12-fold increase in the total area of large pores. Thus, the model simulation suggests that the formation of large pores is responsible for the increases in measured monolayer permeability.

TABLE 1 Results of a two-pore model of epithelial monolayer permeability for unstretched cells or stretched cells

	No stretch	With stretch					
		0.25 Hz				1.0 Hz	
		0–25%	12–25%	0–37%	25–37%	0–25%	0–37%
Small pores							
Radius Å	3.06	3.04	3.44	2.649	3.44	3.44	3.44
Billions of pores n	636	889	401	3370	616	572	1070
Pore area $\times 10^9$ nm^2	187	258	149.1	743	229	212	398
Large pores							
Radius Å	31.2	31.2	27.5	39.6	35.7	33.4	40.5
Thousands of pores n	444	579	782	6070	5990	4820	10310
Pore area $\times 10^6$ nm^2	13.59	17.65	18.59	299	240	168.7	532

The pore model was also used to interpret the permeability data from the PEEP studies at 0.25 Hz (fig. 4). Stretch to peak amplitude of 25% ΔSA (25% and 12–25%; table 1) led to modest increases in total area of small and large pores, and no significant increase in permeability (fig. 4). Stretch to peak magnitude of 37% ΔSA (37% and 25–37%; table 1) produced increases in total area occupied by small pores, and dramatically larger increases in the total area occupied by large pores (18- to 22-fold increases above unstretched monolayers). Again, these data concur with a correlation between significant increases in monolayer permeability (fig. 4) and the total area of the large pores. Finally, the large pore area changes also demonstrate that stretch to a magnitude of 37% ΔSA produces profound large pore area change, even with reduced stretch amplitude.

DISCUSSION

It has previously been shown that subjecting cultured alveolar epithelial cell monolayers to large cyclic stretch for 1 h and a rate of 0.25 Hz increases paracellular tracer flux [8]. Specifically, the current authors found that increasing stretch oscillation amplitude increased monolayer permeability in a nonlinear manner, such that amplitudes around TLC produced dysfunction. The present study examined the effect of increased cycling frequency (1.0 Hz), and separately addressed the influence of stretch oscillation amplitude and peak stretch magnitude on epithelial permeability. The current results indicate that within the physiological range, both the peak stretch magnitude and the cycling frequency affect the extent of stretch-induced barrier dysfunction. Specifically, a reduction in stretch oscillation, while maintaining the same peak stretch magnitude, did not produce significant functional improvements. Combined with the outcomes of a previous study [8], it can now be concluded that the maximum magnitude of stretch rather than SOA (difference between the maximum and minimum stretch in the cycle, equivalent to V_T) produces epithelial barrier dysfunction in sustained cyclic or tonic (0 Hz) mechanical stretch environments. Furthermore, the present authors demonstrated that brief exposure to the same peak stretch magnitude (similar to a deep sigh) does not alter barrier properties. These findings show that caution should be exercised when using large PEEP levels in conjunction with even small V_T, because repetition of high peak deformations could result. The data at large peak stretch levels support the analysis of HAGER *et al.* [27], which evaluated animal and clinical data and reported significant reductions in mortality by decreasing peak inspiratory plateau pressure. However, HAGER *et al.* [27] also noted further reductions in mortality by reducing V_T at high plateau pressures, and more modest effects at lower peak pressures. Perhaps differences between *in vitro* and *in vivo* platforms are due to differences in the readout, namely permeability *versus* mortality.

The observed frequency dependence of cell monolayer permeability is comparable to cell death results, as reported by TSCHUMPERLIN *et al.* [11], in which post-stretch cell viability in 5 day rat alveolar epithelial cells was measured using a plasma membrane rupture assay. In that study, cell death after stretch at 50% ΔSA increased as the applied stretch frequency was increased. However, TSCHUMPERLIN *et al.* [11] observed no significant cytotoxicity with high-deformation magnitudes to 100% TLC, as long as the frequency of stretch remained small (0.25 Hz). The present study has shown that barrier function in the same cultured monolayer preparation is compromised by high peak-deformation magnitude even at modest stretch frequency (0.25 Hz). Thus, it was found that stretch thresholds for barrier dysfunction are lower than those for cell death.

The differing effect of stretch frequency on cell death and epithelial permeability may be due to cellular regulation of the plasma membrane. As inferred by capacitance data presented by FISHER *et al.* [28], the plasma membrane of cultured alveolar epithelial cells is enlarged *via* lipid trafficking within 5 min of the application of 0 Hz stretch to peak basal membrane deformations of 25% ΔSA. It is most likely the case that as stretch frequency increases, the rate of lipid trafficking to the cell membrane is not high enough to support large magnitudes of deformation, which leads to membrane rupture and cell death. Furthermore, the present authors have shown that at a stretch magnitude of 25% ΔSA and all frequencies, the actin cytoskeleton is reorganised with a concentration at cortical cell boundaries [29]. Therefore, it is speculated that increases in paracellular permeability without increases in cell mortality at low stretch frequencies could be explained by a sufficient rate of lipid insertion into the plasma membrane to limit cell death;

however, concurrent rearrangement of the actin cytoskeleton and junctional proteins result in functional alterations, such as permeability increases.

Alternatively, high-frequency cyclic stretch could lead to increases in epithelial permeability through mechanical failure of the cell–cell junction. As cycling frequency increases, the rate of cellular stretch increases and magnifies the forces experienced by the cells and their junctions in a nonlinear manner, owing to the viscoelastic nature of the cells. It is possible that at higher frequencies there is a higher incidence of cell death, which could lead to the formation of holes in the monolayer. The present authors performed live/dead staining on a small number of stretched monolayers, and while there were a higher percentage of dead cells in monolayers stretched at a higher frequency, the dead cells were still adherent to the monolayer, but may have dissociated from neighbouring cells. Previous studies have shown that the loss of junctional integrity leads to increases in permeability similar to stretch at 0.25 Hz to 37% ΔSA, but the monolayer is still significantly less permeable than bare membrane [8]. Therefore, a second mechanism underlying stretch-induced barrier dysfunction could be a mechanical failure of the cell–cell junction due to the development of high viscous forces produced by the increased cycling frequency.

A methological limitation of the current study may be the possible recovery or worsening properties of the epithelial barrier during the 2-h time period between stretch completion and the end of the transport tests. Although proteins in stable junctional complexes have been shown to cycle from the cytoplasm to the membrane in minutes [30], others demonstrate a 4-h lag time between a calcium switch to initiate barrier formation, and development of functioning barriers in Madin-Darby canine kidney cells [31]. In a previous study, the permeability of the monolayers was monitored every 15 min for 2 h following stretch and no significant change in monolayer permeability was found over the time period [8]. Thus, it is unlikely that the junctions undergo significant repair or deterioration during the 2-h period of measurement.

A second limitation is that the period of study was only 60 min, focusing on acute changes in barrier function. In contrast, mechanical ventilation is usually employed for hours or days at a time in the clinical setting, providing a longer time period over which epithelial dysfunction could develop. While changes after 1 h of applying some stretch regimens were observed, it may be possible that the regimens that did not produce any measurable changes in the 1-h stretch period may produce significant barrier disruption after a longer stretch duration. Conversely, it is possible that the cells will adapt to the applied stretch conditions over prolonged stretch periods. In this case, a reduction of epithelial permeability following epithelial adaptation would be expected. The contribution of longer stretch durations should be addressed in future studies. Finally, the relationships between TLC and epithelial deformation used in the present study are based on data obtained by deflating isolated lungs from TLC in a quasi-static manner prior to fixation. It is possible that dynamic lung ventilation *in situ* alters the spatial distribution and magnitude of alveolar epithelial stretch magnitude.

In summary, a homogeneous alveolar epithelial cell monolayer was used to identify limits of end-expiratory volume, stretch magnitude and frequency associated with acute changes in epithelial barrier function. The present data provide a foundation of functional thresholds that can be used in the future to develop experimental designs for the investigation of the mechanics underlying stretch-induced epithelial disruption.

REFERENCES

1 Webb HH, Tierney DF. Experimental pulmonary edema due to intermittent positive pressure ventilation with high inflation pressures. Protection by positive end-expiratory pressure. *Am Rev Respir Dis* 1974; 110: 556–565.
2 The Acute Respiratory Distress Syndrome Network. Ventilation with lower tidal volumes as compared with traditional tidal volumes for acute lung injury and the acute respiratory distress. *N Engl J Med* 2000; 342: 1301–1308.
3 Brower RG, Lanken PN, MacIntyre N, *et al.* Higher *versus* lower positive end-expiratory pressures in patients with the acute respiratory distress syndrome. *N Engl J Med* 2004; 351: 327–336.
4 Levy MM. PEEP in ARDS–how much is enough? *N Engl J Med* 2004; 351: 389–391.
5 Lubman RL, Kim KJ, Crandall ED. Alveolar epithelial barrier properties. *In*: Crystal RG, West JB, eds. The Lung: Scientific Foundations. Philadelphia, Lippincott-Raven, 1997; pp. 585–602.
6 Tschumperlin DJ, Margulies SS. Alveolar epithelial surface area-volume relationship in isolated rat lungs. *J Appl Physiol* 1999; 86: 2026–2033.
7 Tschumperlin DJ, Margulies SS. Equibiaxial deformation-induced injury of alveolar epithelial cells *in vitro*. *Am J Physiol* 1998; 275: L1173–L1183.
8 Cavanaugh JrKJ, Cohen TS, Margulies SS. Stretch increases alveolar epithelial permeability to uncharged micromolecules. *Am J Physiol Cell Physiol* 2006; 290: C1179–C1188.
9 Egan EA. Lung inflation, lung solute permeability, and alveolar edema. *J Appl Physiol* 1982; 53: 121–125.
10 Egan EA. Response of alveolar epithelial solute permeability to changes in lung inflation. *J Appl Physiol* 1980; 49: 1032–1036.
11 Tschumperlin DJ, Oswari J, Margulies AS. Deformation-induced injury of alveolar epithelial cells. Effect of frequency, duration, and amplitude. *Am J Respir Crit Care Med* 2000; 162: 357–362.
12 Agostoni E, Mead J. Statics of the respiratory system. *In*: Wallace O, Fenn HR, eds. Handbook of Physiology: Respiration. Washington, American Physiological Society, 1964; pp. 387–410.
13 Dobbs LG, Gonzalez R, Williams MC. An improved method for isolating type II cells in high yield and purity. *Am Rev Respir Dis* 1986; 134: 141–145.
14 Cheek JM, Evans MJ, Crandall ED. Type I cell-like morphology in tight alveolar epithelial monolayers. *Exp Cell Res* 1989; 184: 375–387.
15 Dobbs LG, Williams MC, Gonzalez R. Monoclonal antibodies specific to apical surfaces of rat alveolar type I cells bind to surfaces of cultured, but not freshly isolated, type II cells. *Biochim Biophys Acta* 1988; 970: 146–156.

16 Qiao R, Zhou B, Liebler JM, Li X, Crandall ED, Borok Z. Identification of three genes of known function expressed by alveolar epithelial type I cells. *Am J Respir Cell Mol Biol* 2003; 29: 98–105.

17 Wang F, Daugherty B, Keise LL, *et al.* Heterogeneity of claudin expression by alveolar epithelial cells. *Am J Respir Cell Mol Biol* 2003; 29: 62–70.

18 Cheek JM, Kim KJ, Crandall ED. Tight monolayers of rat alveolar epithelial cells: bioelectric properties and active sodium transport. *Am J Physiol* 1989; 256: C688–C693.

19 Kim KJ, Borok Z, Ehrhardt C, Willis BC, Lehr CM, Crandall ED. Estimation of paracellular conductance of primary rat alveolar epithelial cell monolayers. *J Appl Physiol* 2005; 98: 138–143.

20 Stahl WR. Scaling of respiratory variables in mammals. *J Appl Physiol* 1967; 22: 453–460.

21 Protein Data Bank. Molecular visualization freeware. www.umass.edu/microbio/rasmol/ Date last updated: July 2008.

22 Kim KJ, Crandall ED. Effects of lung inflation on alveolar epithelial solute and water transport properties. *J Appl Physiol* 1982; 52: 1498–1505.

23 Kim KJ, LeBon TR, Shinbane JS, Crandall ED. Asymmetric [^{14}C]albumin transport across bullfrog alveolar epithelium. *J Appl Physiol* 1985; 59: 1290–1297.

24 Zar J. Biostatistical Analysis. Upper Saddle River, Prentice Hall, 1999.

25 Berg MM, Kim KJ, Lubman RL, Crandall ED. Hydrophilic solute transport across rat alveolar epithelium. *J Appl Physiol* 1989; 66: 2320–2327.

26 Kim KJ, Crandall ED. Heteropore populations of bullfrog alveolar epithelium. *J Appl Physiol* 1983; 54: 140–146.

27 Hager DN, Krishnan JA, Hayden DL, Brower RG, ARDS Clinical Trials Network. Tidal volume reduction in patients with acute lung injury when plateau pressures are not high. *Am J Respir Crit Care Med* 2005; 172: 1241–1245.

28 Fisher JL, Levitan I, Margulies SS. Plasma membrane surface increases with tonic stretch of alveolar epithelial cells. *Am J Respir Cell Mol Biol* 2004; 31: 200–208.

29 Margulies SS, Cavanaugh KC, Cohen TS, Di Paolo BC. High stretch cycling rates alter alveolar epithelial permeability and actin organization. American Thoracic Society International Conference, 2005. San Diego, USA. Volume 2. A826.

30 Shen L, Weber CR, Turner JR. The tight junction protein complex undergoes rapid and continuous molecular remodeling at steady state. *J Cell Biol* 2008; 181: 683–695.

31 Zheng B, Cantley LC. Regulation of epithelial tight junction assembly and disassembly by AMP-activated protein kinase. *Proc Natl Acad Sci USA* 2007; 104: 819–822.